DALTON
FULL PAPER

High-nuclearity $[Pd_{13}Ni_{13}(CO)_{34}]^{4-}$ containing a 26-atom $Pd_{13}Ni_{13}$ core with an unprecedented five-layer close-packed triangular stacking geometry: possible substitutional Pd/Ni crystal disorder at specific intralayer nickel sites †

Nguyet T. Tran, Masaki Kawano, Douglas R. Powell and Lawrence F. Dahl *

Department of Chemistry, University of Wisconsin-Madison, Madison, WI 53706, USA

Received 8th June 2000, Accepted 30th August 2000
First published as an Advance Article on the web 18th October 2000

$[Pd_{13}Ni_{10}(Ni_{3-x}Pd_x)(CO)_{34}]^{4-}$ **1** has been prepared in essentially quantitative yields (>90%) from room-temperature reactions of $[Ni_6(CO)_{12}]^{2-}$ with either $Pd(OAc)_2$ in DMF or $Pd(MeCN)_4(BF_4)_2$ in DMSO. The crystal structure of **1** as the $[PPh_4]^+$ salt was determined from low-temperature CCD X-ray crystallographic analyses of three crystals. **1** was also characterized by elemental analysis, IR, ^{1}H NMR, and electrochemical (CV) measurements. Its structurally unprecedented 26-atom metal polyhedron consists of a 5-layer close-packed triangular stacking arrangement of pseudo-C_{3v} symmetry with an [a(Ni)b(Ni_3)c(Pd_6)a(Pd_7Ni_3)c(Ni_3M_3)] sequence. The overall geometry of the 20-atom ν_3 tetrahedral $Pd_{13}Ni_7$ framework in the top four ccp layers is analogous to the pseudo-T_d cubic geometry of the metal-core previously found in $[Pd_{16}Ni_4(CO)_{22}(PPh_3)_4]^{2-}$ and $[Os_{20}(CO)_{40}]^{2-}$. Each M in the bottom fifth Ni_3M_3 layer denotes an inner triangular atomic site where a substitutional Pd/Ni crystal disorder may occur; the *composite* composition of the three M sites corresponds to $Ni_{3-x}Pd_x$ with $x = 0.45$ for crystal **A** and 0 for **B** and **C**. We thereby formulate **1** to possess a stoichiometric $Pd_{13}Ni_{13}$ core even though crystallographic evidence from crystal **A** indicates the existence of a crystal disorder involving a *small* substitution of Pd for Ni at two of the three inner atomic M sites within the Ni_3M_3 layer. The entire geometry of **1** (including the 34 carbonyl ligands) ideally conforms to C_{3v} trigonal symmetry. A qualitative structure/bonding analysis was performed in order to correlate the geometry of **1** with its electron count. The maximum metal-core diameter is *ca.* 0.87 nm parallel and 0.56 nm perpendicular to the principal 3-fold axis.

Introduction

High-nuclearity transition metal clusters (*i.e.* those arbitrarily designated by us to contain at least 10 metal-core atoms with direct metal–metal bonding) are of considerable current interest because their special intermediate positions at the diffuse boundary between monometallic species and colloidal/bulk metals may possibly result in unusual physical properties due to quantum-size effects.[1] Such ligand-stabilized metal clusters possess an important advantage over both naked and ligand- or polymer-supported colloidal metal clusters in having a well defined geometry and normally being monodispersed. The ligand coordination to large metal cores of clusters may model ligand coordination on metal surfaces.[2] High-nuclearity metal clusters may also produce facile multicenter transformations of small molecules and thereby function in an analogous fashion to homogeneous and heterogeneous metal catalysts.[3] Heterometallic carbonyl clusters are especially useful as precursors for obtaining decarbonylated support-attached species for heteronuclear interactions and bifunctional catalysis.[3,4] For instance, the SiO_2-supported $[Pd_6Fe_6H(CO)_{24}]^{3-}$ trianion was used to generate a Pd–Fe bimetallic catalyst that exhibited high selectivity toward methanol synthesis from CO/H_2 reaction.[5] In general, heterometallic species usually have higher catalytic activity and chemicoselectivity than either of their metal constituents as separate entities. Prime examples are: (1) $PdNi_x$ alloys encaged in NaY zeolite are more selective in promoting CO hydrogenation than either monometallic Pd/NaY and Ni/NaY samples or their physical mixtures;[6] (2) palladium–nickel colloids containing 40–80% Pd, prepared from the reduction of palladium and nickel salts by ethylene glycol at high temperature, have much higher catalytic activities in the hydrogenation of nitrobenzene to aniline than both palladium and nickel monometallic clusters;[7] (3) experimental/theoretical studies[8] of palladium films supported over Ni(111) surfaces showed that the electronic perturbation of Pd atoms produces a striking catalytic efficiency toward the hydrogenation of butadiene.

We are especially interested in nanosized heterometallic clusters containing palladium because they are of potential technological importance in the design of new materials with useful catalytic, electronic, magnetic, optical, and photochemical/electrochemical behavior.[9] Palladium as the bulk metal or contained in compounds, alloys, and clusters is widely utilized as homogeneous/heterogeneous catalysts[6–8,10] or as catalytic precursors[11] in many organic reactions. In addition, palladium metal has been utilized for hydrogen isotope separation, purification, and storage of tritium for over 20 years.[12]

Prior to our research, only a few high-nuclearity heterometallic palladium carbonyl clusters had been prepared and crystallographically characterized. These include the isostructural but electronically non-equivalent $[Pd_6Fe_6(CO)_{24}H]^{3-}$ trianion[13] and $[Pd_6Ru_6(CO)_{24}]^{2-}$ dianion,[13b] the $[Pd_{14}Au_2(CO)_9(PMe_3)_{11}]^{2+}$ dication,[14] and subsequently the electronically equivalent and structurally analogous neutral $Pd_6Os_5(CO)_{19}(dppm)_2$ and $Pd_6Os_5H_2(CO)_{18}(dppm)_2$.[15] Over the past five years we have prepared, isolated, crystallized, and stereophysically characterized a number of new high-nuclearity close-packed heterometallic palladium clusters, which include the $[Pd_{33}Ni_9(CO)_{41}(PPh_3)_6]^{4-}$ tetraanion,[16] the $[Pd_{16}Ni_4(CO)_{22}(PPh_3)_4]^{2-}$ dianion,[16b] the tentatively formulated $[Pd_{30-x}Ni_x(CO)_y]^{4-}$ tetra-

† Dedicated to Professor Sheldon Shore, a remarkable boron/transition metal cluster chemist and good friend, on the occasion of his 70th birthday.

 DOI: 10.1039/b004595k

anion ($x \approx 14$; $y \approx 36$),[17] the $[Pd_7Ni_{18}(CO)_{33}]^{4-}$ and $[Pd_{16}Ni_{16}(CO)_{40}]^{4-}$ tetraanions,[18] the $[Pd_{19.2}Ni_{22.8}(CO)_{48}]^{6-}$ hexaanion,[19] and the neutral $[Pd_{28}(PtPMe_3)(PtPPh_3)_{12}H_{12}(CO)_{27}]$.[20]

Since the phase diagram of the binary Pd–Ni intermetallic system consists at room temperature of a continuous solid solution,[21] it is remarkable that complete segregation of Ni and Pd atoms occurs in all metal-core sites in the above-mentioned Pd–Ni carbonyl clusters,[16,18,19] except possibly for the $Pd_{30-x}Ni_x$ cluster[17] (*i.e.* there is no crystallographic evidence of a substitutional Pd/Ni crystal disorder at any atomic metal site). However, the recently reported trimetallic $[Au_6Pd_6(Pd_{6-x}Ni_x)Ni_{20}(CO)_{44}]^{6-}$ hexaanion[22] possesses a non-stoichiometric 38-atom $Au_6Pd_6(Pd_{6-x}Ni_x)Ni_{20}$ nanosized core (where x was determined from least-squares analyses of X-ray data for *seven* crystals to vary from 2.1 to 5.5). A salient structural feature is that the substitutional Pd/Ni crystal disorder occurs at only six specific non-adjacent pseudoequivalent atomic sites.[22]

Herein, we report two reproducible preparative pathways under controlled, mild conditions that produce in high yields another large bimetallic close-packed Pd–Ni cluster, $[Pd_{13}Ni_{13}(CO)_{34}]^{4-}$ **1**. Its initial formulation with a non-stoichiometric 26-atom $Pd_{13}Ni_{10}(Ni_{3-x}Pd_x)$ core ($x = 0.45$) was based upon a crystallographic least-squares analysis of X-ray data from a crystal **A** which pointed to a relatively *small* but yet detectable replacement of Ni with Pd atoms at two of three pseudoequivalent atomic sites within the bottom basal v_2 triangular Ni_6 layer. Since subsequent X-ray crystallographic examinations of two other crystals **B** and **C** from different preparations showed no evidence of any substitutional Pd/Ni crystal disorder at these intralayer sites (*i.e.* $x = 0$), **1** is thereby formulated to possess a stoichiometric $Pd_{13}Ni_{13}$ core. Details of the particular microscopic crystal disorder found in crystal **A** and resulting implications are presented. This anion **1** as the $[PPh_4]^+$ salt was also characterized by elemental analysis and by IR, ^{1}H NMR, and electrochemical (CV) measurements.

One major goal of our research is to provide reproducible preparative pathways under controlled conditions to produce high-nuclearity metal clusters in reasonably good yields (by optimization of the boundary conditions) to enable physical/chemical studies. In this case the $[Pd_{13}Ni_{13}(CO)_{34}]^{4-}$ tetraanion **1**, isolated in essentially quantitative yields (>90%), has been utilized as a precursor in reactions with trialkylphosphines to generate other intriguing high-nuclearity Pd–Ni and Pd carbonyl phosphine clusters.[23]

A recent report by Longoni and co-workers[24] presents the preparation of $[Pd_{16}Ni_{16}(CO)_{40}]^{4-}$ and $[Pd_{20}Ni_{26}(CO)_{54}]^{6-}$ and the crystallographic characterization of the tetraanion as the tetra-n-butylammonium salt.

Results and discussion

Synthesis of the tetraanion 1

This cluster was isolated in high yields (>90%) from two different preparative methods. Each involved the use of $[Ni_6(CO)_{12}]^{2-}$ as both the reductant and source of Ni and CO. However, these two methods differ with respect to the palladium(II) precursor, the solvent, and the Pd : Ni equivalent reactant ratio; whereas method 1 utilizes $Pd(OAc)_2$, DMF, and a Pd : Ni ratio of 1 : 3, method 2 uses $Pd(MeCN)_4(BF_4)_2$, DMSO, and a Pd : Ni ratio of 1 : 4.

The fact that these variations in reaction boundary conditions between the two preparative procedures do not impact upon the formation and isolation of compound **1** in high yields deserves the following comments concerning reaction parameters that do influence the formation/isolation of other high-nuclearity Pd–Ni carbonyl clusters (given in the Introduction). First, it should be noted that the two Pd : Ni reactant ratios for methods 1 and 2 are not markedly dissimilar in that both indicate that an appreciable excess of the $[Ni_6(CO)_{12}]^{2-}$ reductant is required. In general, similar variations in the ratios of the Pd/Ni reactants do not dramatically alter the types of Pd–Ni clusters formed but do significantly influence product yields. We normally vary the reactant ratios in a systematic fashion in order to optimize the yield of a given cluster, but in this case did not because of the high yields of **1**. However, the nature of the palladium(II) reactant and solvent are often crucial in other similar reactions involving $[Ni_6(CO)_{12}]^{2-}$. For example, reactions in our laboratory of $Pd(OAc)_2$ with $[Ni_6(CO)_{12}]^{2-}$ in DMSO produced the partially characterized $[Pd_{30-x}Ni_x(CO)_y]^{4-}$ tetraanion ($x \approx 14$; $y \approx 36$),[17] while corresponding reactions with similar Pd : Ni ratios in acetone afforded the $[Pd_{16}Ni_{16}(CO)_{40}]^{4-}$ and $[Pd_7Ni_8(CO)_{33}]^{4-}$ tetraanions,[18] and in DMF produced $[Pd_{13}Ni_{13}(CO)_{34}]^{4-}$ **1**, as reported here. On the other hand, Longoni and co-workers[24] synthesized $[Pd_{16}Ni_{16}(CO)_{40}]^{4-}$ from the reaction of $Pd(SEt_2)_2Cl_2$ with $[Ni_6(CO)_{12}]^{2-}$ in THF. Reactions of $Pd(PPh_3)_2Cl_2$ with $[Ni_6(CO)_{12}]^{2-}$ in DMSO afforded $[Pd_{33}Ni_9(CO)_{41}]^{4-}$ and $[Pd_{16}Ni_4(CO)_{22}(PPh_3)_4]^{2-}$ as the two major products.[16]

It is apparent that the reaction pathways that occur in solution are complex and that changes in even one of the reaction boundary conditions (*i.e.* reagents, solvent, reactant mole ratios, concentrations, temperature, reaction time) may profoundly influence the nature of the isolated products.

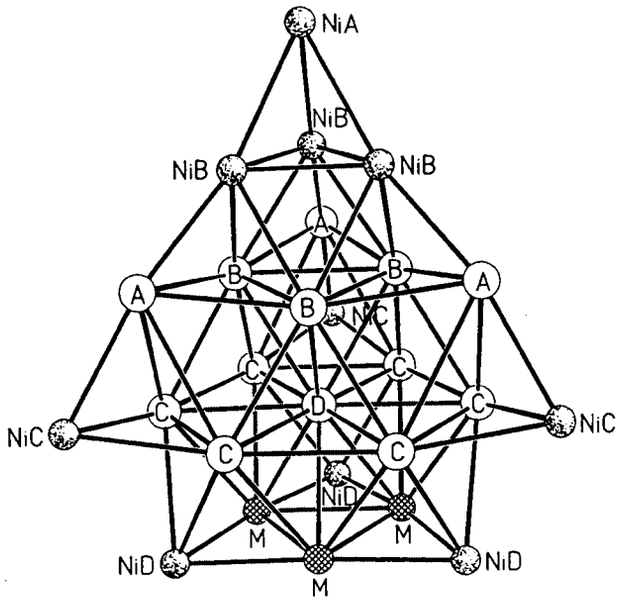

Fig. 1 $Pd_{13}Ni_{10}M_3$ core of $[Pd_{13}Ni_{10}(Ni_{3-x}Pd_x)(CO)_{34}]^{4-}$ **1** with identical labeling under pseudo-C_{3v} trigonal symmetry for symmetry-equivalent metal atoms: Pd (white), Ni (dotted), and M sites (cross-hatched). Its unprecedented 26-atom metal framework may be described as the triangular stacking of five layers in a close-packed [a(Ni)b(Ni_3)c(Pd_6)a(Pd_7Ni_3)c(Ni_3M_3)] sequence. Each M in the inner M_3 triangle of the fifth basal v_2 triangular Ni_3M_3 layer denotes an atomic site where a substitutional Pd/Ni crystal disorder may occur; the composite composition of the three M sites corresponds to $Ni_{3-x}Pd_x$ with $x = 0.45$ for crystal **A** and 0 for crystals **B** and **C**. The resulting non-stoichiometric formulation of $Pd_{13.45}Ni_{12.55}$ for crystal **A** is in accordance with **1** representing the superimposed composite of all co-crystallized individual isomers in the crystal-averaged unit cell of this crystal.

Structure/bonding of $[Pd_{13}Ni_{10}(Ni_{3-x}Pd_x)(CO)_{34}]^{4-}$ 1

(a) Overall configuration. A view of its metallic framework is shown in Fig. 1 and its entire geometry in Fig. 2. The maximum metal-core diameter is *ca.* 0.87 nm parallel and 0.56 nm perpendicular to the principal 3-fold axis. The 26-atom metal-core polyhedron, for which there is no previous example (to our knowledge), may be described as a five-layer close-packed stacking arrangement of pseudo-C_{3v} trigonal symmetry. The top four layers consisting of 13 Pd and 7 Ni atoms are stacked

Table 1 Mean metal–metal connectivities under pseudo-C_{3v} (3m) trigonal symmetry in $[Pd_{13}Ni_{10}(Ni_{3-x}Pd_x)(CO)_{34}]^{4-}$ for crystals **B** ($x = 0$) and **A** ($x = 0.45$) and corresponding individual ranges for **B**[a]

Metal–metal connectivities[b]	N[c]	Mean/Å	Range/Å
Ni(A)–Ni(B)	3	2.70 (2.70)	2.683(1)–2.737(2)
Ni(B)–Ni(B)	3	2.46 (2.45)	2.449(1)–2.460(1)
Ni(C)–Ni(D)	3	3.24 (3.25)	3.214(2)–3.270(2)
Pd(A)–Pd(B)	6	2.84 (2.84)	2.821(1)–2.851(1)
Pd(B)–Pd(B)	3	2.86 (2.85)	2.831(1)–2.892(1)
Pd(A)–Pd(C)	6	3.04 (3.05)	2.966(1)–3.087(1)
Pd(B)–Pd(C)	6	2.74 (2.74)	2.712(1)–2.751(1)
Pd(B)–Pd(D)	3	2.76 (2.76)	2.751(1)–2.762(1)
(Ni-bridged) Pd(C)–Pd(C)	3	2.77 (2.77)	2.759(1)–2.781(1)
(non-Ni-bridged) Pd(C)–Pd(C)	3	2.78 (2.78)	2.761(1)–2.789(1)
Pd(C)–Pd(D)	6	2.77 (2.78)	2.747(1)–2.785(1)
Ni(B)–Pd(A)	3	2.58 (2.58)	2.565(1)–2.601(1)
Ni(B)–Pd(B)	6	2.63 (2.64)	2.613(1)–2.667(1)
Ni(C)–Pd(A)	3	2.59 (2.60)	2.570(1)–2.608(1)
Ni(C)–Pd(C)	6	2.68 (2.69)	2.669(1)–2.696(1)
Ni(D)–Pd(C)	6	2.73 (2.74)	2.693(1)–2.766(1)
M–M	3	2.64 (2.67)	2.635(1)–2.647(1)
M–Ni(D)	6	2.48 (2.50)	2.479(1)–2.495(1)
M–Pd(C)	6	2.74 (2.76)	2.733(1)–2.762(1)
M–Pd(D)	3	2.70 (2.73)	2.699(1)–2.710(1)

[a] The means and individual ranges for symmetry-equivalent distances are for crystal **B**; corresponding means for **A** are given in parentheses. Means for **C** ($x = 0$) agree within 0.01 Å with those for **B**. [b] Atom labeling for the bimetallic core is given in Fig. 1. M designates the three individual symmetry-related atomic sites of the inner Ni_3 triangle within the basal ν_2 Ni_6 triangle that are partially substituted at two of the three individual Ni sites by Pd atoms in crystal **A** but not in **B** and **C**. The value x denotes the *composite* 3-site crystal disorder of the $(3 - x)$Ni/xPd atoms. [c] Denotes the number of symmetry-equivalent metal–metal connectivities under C_{3v} symmetry.

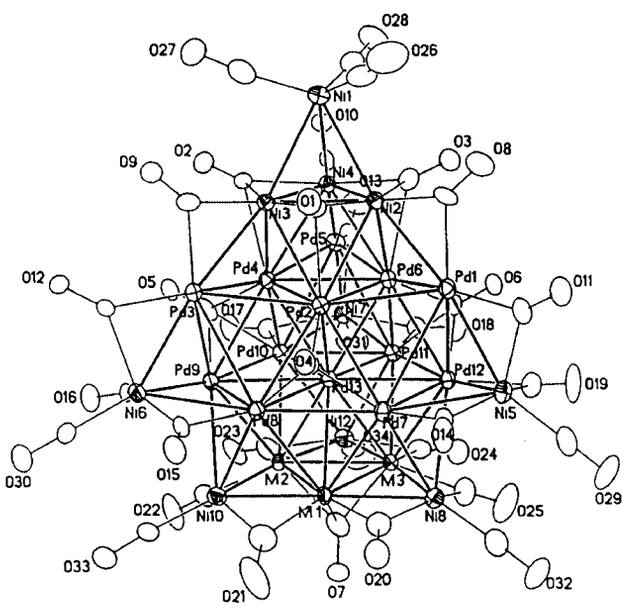

Fig. 2 The entire tetraanion **1** of pseudo-C_{3v} trigonal symmetry with atomic displacement ellipsoids at 50% probabilities. The 34 carbonyl ligands consist of nine Ni-attached terminal COs, 18 doubly bridging COs, and 7 triply bridging COs. The principal threefold axis passes through the top Ni(A), the internal Pd(i) (labeled Pd(D)), and the bottom M_3-attached triply bridging CO.

in a cubic close-packed (ccp) [a(Ni)b(Ni_3)c(Pd_6)a(Pd_7Ni_3)] sequence. The overall geometry of this 20-atom ν_3 tetrahedral metal framework is analogous to the pseudo-T_d cubic geometry of the metal core found in the high-nuclearity $[Pd_{16}Ni_4(CO)_{22}(PPh_3)_4]^{2-}$ dianion **2**,[16b] and $[Os_{20}(CO)_{40}]^{2-}$ dianion **3**.[25] The centered hexagonal Pd_7 fragment of the fourth Pd_7Ni_3 layer in **1** forms a hexagonal close packed (hcp) linkage *via* only direct metal–metal bonding with the fifth 6-atom basal ν_2 triangular Ni_6 layer. The resulting one interior Pd(i) atom in the fourth layer is encapsulated by 12 hcp atoms. This close-packed metal core has 7 octahedral and 15 tetrahedral interior holes. Vertex truncation of this 26-atom polyhedron (Fig. 1) by removal of the Ni(A) atom in the top layer and the three symmetry-equivalent Ni(C) vertices in the fourth Pd_7Ni_3 layer (under C_{3v} symmetry) gives rise to a 22-atom metal polyhedron that is analogous to the Rh_{22} core found in the $[Rh_{22}(CO)_{37}]^{4-}$ tetraanion.[26]

(b) Nature of microscopic crystal disorder in the metal core of crystal A. The formulation of the metal core of compound **1** as $Pd_{13}Ni_{13}$ ($x = 0$) is in harmony with an elemental analysis (see below). Nevertheless, least-squares crystallographic refinement of the X-ray data for crystal **A** revealed that a *small* substitutional Pd/Ni crystal disorder occurs at two of the three independent atomic nickel sites (labeled M in Fig. 1) in the inner Ni_3 triangle of the basal Ni_6 layer. For the initial crystal **A**, *individual* Pd/Ni occupancies of 0.23/0.77, 0.22/0.78, and 0/1.00 were determined (*i.e.* there was no crystallographic evidence of any substitutional disorder at any of the other 24-atom metal sites including the third atomic M site). This non-stoichiometric formulation corresponds to **1** representing the superimposed composite of all co-crystallized stereoisomers of **1** in the crystal-averaged unit cell of a given crystal. It is noteworthy that all crystals in the same sample are not expected to have the same fixed non-stoichiometric composition (*i.e.* the identical composite Pd/Ni substitutional disorder denoted by x) as that in crystal **A**.

X-Ray diffraction analyses were then performed on two other crystals **B** and **C** from different samples. However, their least-squares refinements provided no crystallographic indication of Ni being partially substituted by Pd atoms at any of the three atomic M sites. Hence, it is presumed that compound **1** in all of its crystalline materials is essentially composed of individual $[Pd_{13}Ni_{13}(CO)_{34}]^{4-}$ tetraanions.

(c) Metal–metal connectivities and resulting implications. Since the corresponding mean metal–metal distances under assumed C_{3v} trigonal symmetry for both crystals **B** and **C** (which give rise to the stoichiometric $Pd_{13}Ni_{13}$ core) agree within 0.01 Å, only those for crystals **B** and **A** are presented in Table 1. Differences between the corresponding mean distances for the two crystals are within 0.03 Å; only those for **B** are utilized in this discussion. The corresponding variations of the individual metal–metal distances for each of the means for crystal **B** are also given in Table 1 in order to show the relatively

small dispersion of distances for a given mean under pseudo C_{3v} symmetry.

Of the 36 Pd–Pd bonding connectivities, only six *interlayer* Pd(A)–Pd(C) connectivities (mean, 3.04 Å) are markedly long; the means for the seven other different kinds of Pd–Pd connectivities (under C_{3v} symmetry) show only small variations (maximum, 0.07 Å) from the overall mean of 2.79 Å. This value is close to that of 2.75 Å in ccp palladium metal.[27] The much longer Pd(A)–Pd(C) connectivities are presumably a consequence of deviations from a regular close-packed structure due at least partially to the 0.11 Å difference in covalent radii between the Pd and Ni atoms[28] as well as steric effects arising from the disposition of the carbonyl ligands.

Likewise, the smaller dimensions of the ν_2 Ni_6 triangle in the basal fifth layer relative to those of the ν_3 Pd_7Ni_3 triangle in the fourth layer result in the three *interlayer* Ni(C)–Ni(D) distances (mean, 3.24 Å) being unusually long and essentially non-bonding. Consequently, the adjacent interlayer Ni(C) and Ni(D) atoms are geometrically prevented from forming bonding connectivities even though the entire 26-atom metal core in **1** exhibits a close-packed atomic arrangement. The means of the other non-bridged Ni(A)–Ni(B) and CO-bridged Ni(B)–Ni(B) bond connectivities are 2.70 and 2.46 Å, respectively. The Ni–Ni distance in ccp nickel metal is 2.50 Å.[27]

The five different means for the 24 Pd–Ni bonding connectivities vary from 2.58 to 2.73 Å; this 0.15 Å range is readily attributed to the combined effects of carbonyl ligation and irregular variations within the close-packed atomic lattice. These values are within the normal range of Pd–Ni bonding connectivities found in other Pd–Ni carbonyl clusters.

In Table 1 M designates for crystal **B** the three symmetry-equivalent atomic sites (under assumed C_{3v} symmetry) of the inner Ni atoms within the basal ν_2 triangular Ni_6 layer, while M designates for crystal **A** the three possible substitutional Pd/Ni crystal-disordered atomic sites that correspond to the $Ni_{3-x}Pd_x$ formulation ($x = 0.45$). The observed bonding connectivities of the three M atomic sites to each other (means 2.64 *vs.* 2.67 Å for crystals **B** and **A**), to the three intralayer Ni(D) atoms (means 2.48 *vs.* 2.50 Å), to the six interlayer Pd(C) sites (means 2.74 *vs.* 2.76 Å), and to the interlayer interior Pd(D) atom (means 2.70 *vs.* 2.73 Å) are all self-consistent with respect to the partial substitution of larger Pd for Ni atoms in crystal **A**.

(d) Carbonyl distribution and resulting consequences. The 34 carbonyl ligands in compound **1** consist of 9 Ni-attached terminal COs, 18 doubly bridging COs, and 7 triply bridging COs (Fig. 2). The disposition of these COs enveloping the 26-atom metal core and resulting consequences are as follows: (1) the top-layer Ni(A) has three terminal COs, while each of the other six Ni atoms has one terminal CO; (2) both the second Ni_3 and third Pd_6 layers have only *interlayer* COs. The third Pd_6 layer is connected to each of the adjacent second Ni_3 and fourth Pd_7Ni_3 layers by three edge-bridging and three capping COs; (3) the fourth Pd_7Ni_3 layer additionally has six *intralayer* edge-bridging COs spanning the six Ni(D)–Pd(C) connectivities along its three triangular Ni–Pd–Pd–Ni edges; and (4) the basal ν_2 triangular Ni_3M_3 layer has only *intralayer* carbonyls, namely three Ni-attached terminal COs, six edge-bridging COs spanning the M–Ni(D) connectivities along the three triangular Ni–M–Ni edges, and the one triply bridging CO which caps the three atomic M sites.

This particular CO distribution results in the conformity of its metal–carbonyl connectivities to pseudo-C_{3v} symmetry. The principal threefold axis passes through Ni(A) in the top layer, the internal Pd(D) in the fourth Pd_7Ni_3 layer, and the M_3-capped CO. One important consequence is that the top two Ni and Ni_3 layers and the bottom two Pd_7Ni_3 and Ni_3M_3 layers are solely connected by close-packed metal–metal bonding interactions.

The means of the determined M–CO bond lengths are: Ni–CO, 1.78; Ni–(μ-CO), 1.92; Pd–(μ-CO), 1.99; Ni–(μ_3-CO), 1.96; Pd–(μ_3-CO), 2.37 in the Ni_2Pd-capped COs; and Pd–(μ_3-CO), 2.13 Å in the Pd_3-capped COs. The means of the C–O bond lengths are 1.13 Å for terminal COs, 1.16 Å for μ-COs, and 1.17 Å for μ_3-COs.

(e) Bonding analysis *via* electron-counting schemes. The observed number of metal cluster valence electrons (CVEs) in this close-packed cluster, which may be considered to possess globally delocalized metal–metal bonding, is 332 (*i.e.* 26×10 (Pd,Ni) + 34×2 (CO) + 4 (charge) = 332). The calculated number of CVEs obtained from the use of either the Mingos model[29,30] or Teo/Zhang model[31,32] for close-packed metal clusters is 326. An explanation accounting for this predicted electron count being 6 electrons less than the observed number is that the entire 26-atom metal core does not conform to a close-packed polyhedron in that the three Ni(C) vertices in the fourth Pd_7Ni_3 layer and the corresponding Ni(D) vertices in the basal Ni_3M_3 layer are sufficiently far apart (mean 3.25 Å) that their close-packed connectivities are non-bonding (see above). If these three interlayer pairs of Ni(C) and Ni(D) were connected at shorter bonding Ni(C)–Ni(D) distances to give a fully metal–metal bonded close-packed geometry, it is then presumed that a loss of the terminal CO attached to each of the three Ni(C) atoms, which are tetrahedrally coordinated to four COs, would occur such that the resulting observed electron count of 326 (instead of 332) would then be in agreement with the calculated value. Hence, the observed carbonyl ligation is completely compatible with the fact that the close-packed lattice distortion gives rise to non-bonding Ni(C)–Ni(D) connectivities.

Comparative geometrical analysis of $[Pd_{13}Ni_{10}(Ni_{3-x}Pd_x)(CO)_{34}]^{4-}$ 1, $[Pd_{16}Ni_4(CO)_{22}(PPh_3)_4]^{2-}$ 2, and $[Os_{20}(CO)_{40}]^{2-}$ 3 and implications concerning the different carbonyl dispositions

Formal removal of the basal $Ni_3M_3(CO)_3(\mu\text{-}CO)_6(\mu_3\text{-}CO)$ layer from the tetraanion **1** produces the hypothetical $[Pd_{13}Ni_7(CO)_{24}]$ fragment which has an analogous metal-core framework with that in the $[Pd_{16}Ni_4(CO)_{22}(PPh_3)_4]^{2-}$ dianion **2**. This latter cluster, which was previously prepared and structurally characterized in our laboratories by Kawano *et al.*,[16b] is best described as a 20-atom ccp tetrahedron of pseudo-T_d cubic symmetry containing four metal atoms along each of the six tetrahedral edges with the four Ni atoms located at the four tetrahedral corners. Under T_d symmetry there are four equivalent Pd(A) atoms located at the centers of the four 10-atom tetrahedral Pd_7Ni_3 faces and 12 equivalent Pd(B) atoms distributed as the two inner metal atoms along each of the six tetrahedral Ni–Pd(B)–Pd(B)–Ni edges. The pseudo-T_d $Pd_{16}Ni_4$ core may also be viewed along each of the four symmetry-equivalent threefold axes as a four-layer ccp stacking arrangement composed of individual a(Ni)b(Pd_3)c(Pd_6)a(Pd_7Ni_3) layers. This four-layer ccp sequence only differs from the corresponding sequence in the top four $Pd_{13}Ni_7$ layers in **1** by formal replacement of the Ni_3 triangle in the second layer of **1** with a congeneric Pd_3 triangle in **2**. The ligand polyhedron surrounding the $Pd_{16}Ni_4$ core in **2** consists of four triphenylphosphine groups each terminally coordinated to one of the four corner Ni atoms, four terminal COs each linked to the central Pd(A) atom on each tetrahedral Pd_7Ni_3 face, and 18 doubly bridging COs, of which each spans one of the three adjacent pairs of metal atoms along each of the six tetrahedral Ni–Pd(B)–Pd(B)–Ni edges.

Of particular interest are the observed differences in the disposition of the 24 CO ligands about the hypothetical $Pd_{13}Ni_7$ fragment in the tetraanion **1** *versus* that of the 22 CO/4 PPh_3 ligands about the $Pd_{16}Ni_4$ core in **2**. A comparative analysis reveals the following salient differences.

(1) The top Ni(A) atom in the tetraanion **1** has a trigonal pyramidal ligand array of three terminal COs with only direct Ni–Ni bonding to the adjacent Ni_3 layer, while each of the other three symmetry-equivalent corner Ni(C) atoms has a localized

tetrahedral ligand environment composed of one terminal CO and three edge-bridging COs connecting it to a Pd_3 triangle. In **2** each of the four symmetry-equivalent nickel vertices has a localized tetrahedral ligand environment consisting of the terminal PPh_3 and three edge-bridging COs linking it to the adjacent Pd_3 layer (along with the much weaker Ni–Pd bonding). This difference in localized ligand coordination presumably reflects the combined electronic/steric effects of primarily the bulky electron-donating PPh_3 ligands in **2** coupled with formal replacement of the adjacent second-layer Ni_3 triangle in **1** by the second-layer Pd_3 triangle in **2**.

(2) In the pseudo-T_d $Pd_{16}Ni_4$ core of the dianion **2** each of the six equivalent Ni–Pd–Pd–Ni edges is spanned by three doubly bridging CO ligands. In the corresponding four-layer pseudo-C_{3v} $Pd_{13}Ni_7$ fragment of **1**, 12 doubly bridging COs link the 12 Pd–Ni pairs along the three Ni(A)–Ni(B)–Pd(A)–Ni(C) and three Ni(C)–Pd(C)–Pd(C)–Ni(C) edges, while the six triply bridging COs cap the Pd(B)$Ni(B)_2$ and Pd(B)$Pd(C)_2$ triangles on each of the three symmetry-equivalent Pd_5Ni_5 faces (Fig. 1).

The Os_{20} core of the $[Os_{20}(CO)_{40}]^{2-}$ dianion **3**,[25] which likewise has an analogous ccp ν_3 tetrahedral geometry, is encapsulated by 40 terminal COs, of which three are coordinated to each of the four Os vertices, two to each of the other 12 Os atoms along the six tetrahedral edges, and one to the central atom on each of the four 10-atom tetrahedral faces.

One major consequence of the above different carbonyl arrangements about the geometrically analogous metal frameworks of the anions **1**, **2**, and **3** involves the mode of carbonyl linkage to the central (terrace-like) metal atom on a given 10-atom tetrahedral (111) face. In sharp contrast to one terminal CO being coordinated to the central metal atom on each 10-atom tetrahedral face in **2** and **3**, the central (terrace-like) Pd atom on each of the three triangular Pd_5Ni_5 faces of the pseudo-C_{3v} $Pd_{13}Ni_7$ fragment of **1** is connected to two $PdNi_2$- and Pd_3-capped carbonyl ligands. This latter coordination thereby provides a striking illustration that a terrace-like metal site in a ccp (111) metal surface may be connected to bridging COs instead of one terminal CO, depending upon the types of atoms on the metal surface as well as the extent of CO coverage.

Atomic site preferences in heterometallic systems

(a) Previous studies. The particular geometrical arrangement of different metal atoms in a heterometallic cluster is presumed to reflect differences in the bond-energy capabilities of the different metal constituents. A recent comprehensive review by Miller[33] of atomic site preferences in solid-state intermetallic structures illustrated that theoretical analyses *via* second moment scaling techniques have provided good estimates of the structural energy differences for different atomic arrangements. Such calculations have been highly successful in predicting structure/composition/property relationships in many binary intermetallic compounds.

The phase diagram of the binary Pd–Ni intermetallic system consists of a continuous solid solution at room temperature.[21] Therefore, the isolation of completely segregated Pd/Ni cores (*i.e.* ones without crystallographic evidence of a substitutional Pd/Ni crystal disorder at any atomic site) in the $[Pd_{33}Ni_9(PPh_3)_6(CO)_{41}]^{4-}$ and $[Pd_{16}Ni_4(PPh_3)_4(CO)_{22}]^{2-}$ anions,[16] the $[Pd_7Ni_{18}(CO)_{33}]^{4-}$ tetraanion,[18] and the $[Pd_{16}Ni_{16}(CO)_{40}]^{4-}$ tetraanion,[18,24] must be a consequence of the markedly different coordination behavior of Pd and Ni with the carbonyl/phosphine ligands at each atomic metal site in the resulting bimetallic core.

The trimetallic $[Au_6Pd_6(Pd_{6-x}Ni_x)Ni_{20}(CO)_{44}]^{6-}$ hexaanion[22] contains a non-stoichiometric $Au_6Pd_6(Pd_{6-x}Ni_x)Ni_{20}$ nanosized core, in which a substitutional Pd/Ni crystal disorder was found to occur at only *six* specific non-adjacent pseudo-equivalent atomic M sites (three crystallographically independent); for the *composite* six-site crystal disorder of the $(6 - x)$Pd/xNi atoms, x was determined for *seven* crystals to vary from 2.1 (65% Pd, 35% Ni) to 5.5 (8% Pd, 92% Ni). In order to provide an explanation as to why this particular Pd/Ni substitutional crystal disorder occurs solely at six symmetry-related specific atomic sites as opposed to exclusive occupation of either Au, Pd or Ni atoms at the other 38 atomic metal positions, a qualitative structure/bonding analysis was performed. The results clearly indicate that metal–carbonyl as well as metal–metal bonding must be taken into account in determining site preference effects.[22] In other words, stabilization-energy differences between different metals at each atomic site in a heterometallic carbonyl cluster are critically dependent upon *composite* contributions of both metal–CO and metal–metal bond and site energies. In this connection it has been shown theoretically for CO-bridged metal sites that metal–CO bonding is dominant relative to metal–metal bonding.

In sharp contrast, Teo *et al.*[34] have recently shown that a quantitative model based only on calculated relative metal–metal bond energies can provide correct predictions of the atomic site preferences determined crystallographically for their unparalleled vertex-sharing centered polyicosahedral series of bimetallic (Au–Ag) and trimetallic (Au–Ag–M; M = Ni, Pd or Pt) clusters with phosphine/halide ligands.[35] Their model[34] assumes that metal–metal bonding in a heterometallic stereoisomer is composed of a covalent component and an ionic component which are modeled in the bond-energy calculations by use of cohesive energies and electronegativities, respectively. The distance dependence of the metallic bond energy was estimated by use of the Leonard–Jones potential. Teo *et al.*[34] pointed out that their model, which compares the relative strengths of metal–metal bonds for various stereoisomers, can be applied to other heterometallic transition metal clusters, but only where differences in metal–metal bonding are dominant relative to differences in metal–ligand bonding. Site preference effects of different metals in naked and ligated heterometallic clusters were reported by Mingos and Zhenyang[36] on the basis of their extensive analysis *via* MO perturbation theory.

(b) Possible substitutional Pd/Ni crystal disorder in $[Pd_{13}Ni_{10}(Ni_{3-x}Pd_x)(CO)_{34}]^{4-}$ 1. Single-crystal X-ray diffraction analyses of the initial crystal **A** indicated for its 26-atom bimetallic core that 13 atomic sites are occupied by only Pd atoms and 7 atomic sites by only Ni atoms within the top four layers. Crystallographic least-squares refinement including occupancy factors revealed that in the bottom fifth ν_2 triangular Ni_6 layer two of the three pseudo-equivalent atomic sites within the inner Ni_3 triangle possess a relatively small substitutional crystal disorder involving the replacement of Ni by Pd atoms; the *composite* composition for the three individual M sites was found to be $Ni_{3-x}Pd_x$ with $x = 0.45$ for crystal **A**. The sole presence of either Pd or Ni atoms at the other 23 atomic sites with substitutional Pd/Ni crystal disorder being limited to only the three M sites is related to the extent of dissimilarity of the stabilization-energy differences in the composite metal–metal and metal–carbonyl bonding interactions for the resulting possible stereoisomers. The relative bond-energy strengths of such interactions in the tetraanion **1** are critically dependent upon the metal–metal distances within the distorted close-packed metal-core geometry, whose observed large irregularities are attributed to metal atom-size differences and bond-shortening effects of bridging carbonyl ligands coupled with resulting steric packing influences among the surrounding carbonyl ligands.

The occurrence of only Ni atoms at the seven vertices in the tetraanion **1** is in accordance with the previously determined crystal structures of close-packed Pd–Ni carbonyl clusters.[16,18,19,24] This atomic preference may be rationalized in terms of terminal COs forming much stronger bonding interactions with Ni than with Pd. Persuasive evidence for the terminal Pd–CO bonds being much weaker is given by the paucity of known palladium complexes (and clusters) that have terminal CO

ligands;[16,37,38] of these, a considerable number are not thermally stable and undergo decarbonylation.

The presence of only Ni atoms at the three triangular sites in the second layer of the tetraanion **1** is completely consistent with CO-bridged Ni–Ni connectivities being much stronger (due primarily to Ni–CO bonding) at the observed short intralayer distances (means 2.46 and 2.45 Å for crystals **B** and **A**). However, the means for the other metal–metal connectivities (Table 1) do not permit one to rationalize why substitutional Pd/Ni crystal disorder is found in crystal **A** solely at the M sites in **1**. One can only generalize that its occurrence is a consequence of the resulting overall relative energy stabilities based upon combined metal–metal and metal–CO bond energies *not* being sufficiently different for each individual stereoisomer. In this connection the non-stoichiometric $Pd_{13.45}Ni_{12.55}$ core of **1** in crystal **A** represents the superimposed non-stoichiometric composite of all co-crystallized individual stereoisomers in the crystal-averaged unit cell of this crystal.

Experimental

Syntheses of $[Pd_{13}Ni_{13}(CO)_{34}]^{4-}$ 1 as the $[PPh_4]^+$ salt

(a) Method 1. In a typical reaction, $Pd(OAc)_2$ (0.28 g, 1.20 mmol) was dissolved in 15 mL of DMF and added dropwise over 20–25 min *via* a stainless steel cannula to a stirred solution of $[NMe_4]_2[Ni_6(CO)_{12}]$ (0.50 g, 0.60 mmol) in 15 mL of DMF. The solution changed quickly from cherry red to dark brown without any precipitate being formed. It was stirred at room temperature for 6 hours, after which 4.5 g of PPh_4Br dissolved in 15 mL of MeOH were added *via* a cannula. An ice bath was used to cool the reaction mixture before the addition of 150 mL of distilled/degassed water. A dark brown solid, which precipitated, was separated from the clear solution by filtration. The solid was washed first with MeOH (4 × 50 mL) to remove the excess of PPh_4Br and then with THF (2 × 20 mL) to remove the unchanged $[Ni_6(CO)_{12}]^{2-}$. Extraction of the residue with acetone gave a dark brown material (0.41 g) which was characterized by X-ray diffraction as $[PPh_4]^+_4[Pd_{13}Ni_{10}(Ni_{3-x}Pd_x)(CO)_{34}]^{4-}$ (where $x = 0.45$ for crystal **A** and 0 for **B** and **C**). After the acetone extraction, a small amount of black powder remained. In general, yields of the tetraanion **1** as the $[PPh_4]^+$ salt are >90% based on palladium.

(b) Method 2. A 0.15 g sample of the tetraanion **1** was also prepared from the reaction of $Pd(MeCN)_4(BF_4)_2$ (0.20 g, 0.45 mmol) in 10 mL of DMSO with a mixture of $[NMe_4]_2[Ni_6(CO)_{12}]$ (0.25 g, 0.30 mmol) in 10 mL of DMSO and $Me_3NO{\cdot}2H_2O$ (0.07 g, 0.60 mmol) in 5 mL of DMSO. The reaction was allowed to continue for 2 days at room temperature, after which the product was isolated as described in method 1. High yields (>90%) were again obtained based on palladium.

X-Ray diffraction analyses

Crystallographic data are given for three crystals **A**, **B**, and **C** selected from different samples.

Crystals from each sample were grown as dark brown, thin plates by the slow-diffusion technique. The sample was dissolved in acetone and MeCN (1 : 1 ratio) and then layered with diisopropyl ether in the dark in order to grow crystals (*i.e.* long exposure to light led to the formation of an uncharacterized, oily product). Intensity data were collected at −140 °C *via* a SMART CCD area detector system mounted on a Siemens P4 diffractometer with graphite-monochromated Mo-Kα radiation from a standard sealed-tube generator. An empirical absorption correction (SADABS)[39] was applied to each data set (for Mo-Kα: crystal **A**, $\mu = 3.648$ mm^{-1}; crystals **B** and **C**, $\mu = 3.625$ mm^{-1}). The structural determination was obtained by use of direct methods. Anisotropic least-squares refinement (based on F^2) was performed with SHELXTL.[40] A centrosymmetrically disordered solvated acetonitrile molecule lies on one inversion center in the triclinic unit cell.

(1) Crystal A. $[PPh_4]^+_4[Pd_{13}Ni_{10}(Ni_{3-x}Pd_x)(CO)_{34}]^{4-}{\cdot}0.5$MeCN, $x = 0.45$; $M = 4498.48$, triclinic, space group $P\bar{1}$, $a = 17.226(1)$, $b = 17.937(1)$, $c = 22.828(1)$ Å, $\alpha = 82.433(2)$, $\beta = 87.584(2)$, $\gamma = 70.599(2)°$, $V = 6595.00(3)$ Å^3, $Z = 2$. A sphere of 41 393 data was collected *via* 0.3 φ scans over a 2θ range of 3.60–50.00°. Refinement (1761 parameters/7 restraints for solvent) on 22 169 independent merged reflections ($R_{int} = 0.039$) converged at $wR2(F^2) = 0.110$ for all data; $R1(F) = 0.043$ for 18 263 observed data ($I > 2\sigma(I)$).

(2) Crystal B. $[PPh_4]^+_4[Pd_{13}Ni_{13}(CO)_{34}]^{4-}{\cdot}0.5$MeCN, $M = 4476.78$, triclinic, space group $P\bar{1}$, $a = 17.205(3)$, $b = 18.061(3)$, $c = 22.922(4)$ Å, $\alpha = 82.306(3)$, $\beta = 87.368(3)$, $\gamma = 70.283(3)°$, $V = 6645(2)$ Å^3, $Z = 2$. A sphere of 35 088 data was collected *via* 0.3 ω scans over a 2θ range of 3.52–50.00°. Refinement (1774 parameters/79 restraints on the positional and the displacement parameters of the solvent atoms, and the displacement parameters of four other light atoms) on 23,018 independent merged reflections ($R_{int} = 0.047$) converged at $wR2(F^2) = 0.149$ for all data; $R1(F) = 0.050$ for 17 604 observed data ($I > 2\sigma(I)$).

(3) Crystal C. $[PPh_4]^+_4[Pd_{13}Ni_{13}(CO)_{34}]^{4-}{\cdot}0.5$MeCN, $M = 4476.78$, triclinic, space group $P\bar{1}$, $a = 17.206(2)$, $b = 18.040(2)$, $c = 22.930(3)$ Å, $\alpha = 82.320(2)$, $\beta = 87.301(2)$, $\gamma = 70.260(2)°$, $V = 6639.0(14)$ Å^3, $Z = 2$. A sphere of 35 779 data was collected *via* 0.3 ω scans over a 2θ range of 3.52–50.00°. Refinement (1774 parameters/43 restraints on the positional and the displacement parameters of the solvent atoms, and the displacement parameters of two other light atoms) on 23 076 independent merged reflections ($R_{int} = 0.069$) converged at $wR2(F^2) = 0.274$ for all data; $R1(F) = 0.066$ for 17 669 observed data ($I > 2\sigma(I)$).

CCDC reference number 186/2171.

See http://www.rsc.org/suppdata/dt/b0/b004595k/ for crystallographic files in .cif format.

Elemental analysis and spectroscopic/electrochemical characterization of $[Pd_{13}Ni_{10}(Ni_{3-x}Pd_x)(CO)_{34}]^{4-}$ 1 as the $[PPh_4]^+$ salt

An elemental analysis was performed by Desert Analytics (Tucson, AZ) on a crystalline sample. Calculated values are for $[PPh_4]^+_4[Pd_{13}Ni_{13}(CO)_{34}]^{4-}{\cdot}0.5$MeCN. Calculated (found): C, 35.14 (34.34); H, 1.83 (1.79); N, 0.16 (0.21); Ni, 17.04 (16.82); Pd, 30.90 (30.99)%. The agreement between corresponding calculated and observed percentages is good for each element. The elemental analysis does not allow one to discriminate between the stoichiometric $[Pd_{13}Ni_{13}(CO)_{34}]^{4-}$ formulation ($x = 0$ for crystals **B** and **C**) and the crystallographically determined non-stoichiometric formulation ($x = 0.45$ for **A**).

An IR spectrum (MeCN) of $[(PPh_4)_4][Pd_{13}Ni_{13}(CO)_{34}]$ exhibited absorption maxima at 2027(vs) and 2001(sh) cm^{-1} for terminal carbonyls and at 1911(sh), 1887(s), and 1859(s) cm^{-1} for bridging carbonyls. A ^{1}H NMR spectrum of **1** (500 MHz, CD_3CN, 23 °C) did not reveal any resonances which could be ascribed to hydride species. A ^{13}C NMR spectrum (126 MHz, CD_3CN) gave signals corresponding to only the $[PPh_4]^+$ counter ions; resonances characteristic of the carbonyl ligands were not detected either at room temperature or at −30 °C.

Cyclic voltammograms were obtained *via* a BAS-100 Electrochemical Analyzer with the electrochemical cell enclosed in a nitrogen-filled atmosphere glove box. At 50 mV s^{-1} scan rate in acetonitrile (0.1 M NBu_4PF_6 as supporting electrolyte) at a platinum disk working electrode, two broad irreversible oxidation waves at *ca.* 0.1–0.4 and 1.3 V and two broad irreversible reduction waves at *ca.* −0.5 and −1.9 V (*vs.* SCE) were observed.

Acknowledgements

This research was supported by the National Science Foundation. Departmental purchase of the CCD area detector system in 1995 was made possible by funds from the NSF (Grant CHE-9310428) and the UW-Madison Graduate School and Chemistry Department.

References

1 L. J. de Jongh, in *Physics and Chemistry of Metal Cluster Compounds*, ed. L. J. de Jongh, Kluwer Academic Publishers, Dordrecht, 1994, ch. 1, p. 1; R. E. Benfield, *J. Phys. Chem.*, 1987, **91**, 2712 and references therein; D. A. van Leeuwen, J. M. van Ruitenbeek, L. J. de Jongh, A. Ceriotti, G. Pacchioni, O. D. Häberlen and N. Rösch, *Phys. Rev. Lett.*, 1994, **73**, 1432; M. P. Cifuentes, M. G. Humphrey, J. E. McGrady, P. J. Smith, R. Stranger, K. S. Murray and B. Moubaraki, *J. Am. Chem. Soc.*, 1997, **119**, 2647 and references therein; J. L. Coffer, J. R. Shapley and M. G. Drickamer, *J. Am. Chem. Soc.*, 1990, **112**, 3736; J. S. Bradley, E. W. Hill, C. Klein, B. Chaudret and A. Duteil, *Chem. Mater.*, 1993, **5**, 254.

2 E. L. Meutterties and R. M. Wexler, *Surv. Prog. Chem.*, 1983, **10**, 61; G. A. Somorjai, *Introduction to Surface Chemistry and Catalysis*, Wiley-VCH, New York, 1994.

3 R. D. Adams, in *Metal–Metal Bonds and Clusters in Chemistry and Catalysis*, ed. J. P. Jr. Frackler, Plenum Press, New York, 1990, p. 75; D. J. Darensbourg, in *Metal–Metal Bonds and Clusters in Chemistry and Catalysis*, ed. J. P. Jr. Frackler, Plenum Press, New York, 1990, p. 41; L. H. Pignolet, M. A. Aubart, K. L. Craighead, R. A. T. Gould, D. A. Krogstad and J. S. Wiley, *Coord. Chem. Rev.*, 1995, **143**, 219 and references therein; P. Braunstein and J. Rosé, in *Stereochemistry of Organometallic and Inorganic Compounds*, ed. I. Bernal, Elsevier, Tarrytown, NY, 1988, vol. 3; *Catalysis by Di- and Polynuclear Metal Cluster Complexes*, eds. R. D. Adams and F. A. Cotton, Wiley-VCH, New York, 1998, pp. 1–555.

4 M. Ichikawa, *Adv. Catal.*, 1992, **38**, 283 and references therein.

5 T. Kimura, A. Fukuoka, A. Fumagalli and M. Ichikawa, *Catal. Lett.*, 1989, **2**, 227.

6 J. S. Feeley, A. Yu Stakheev, A. P. Cavalcanti and W. M. H. Sachtler, *J. Catal.*, 1992, **136**, 182; J. S. Feeley and W. M. H. Sachtler, *J. Catal.*, 1991, **131**, 573.

7 N. Toshima and P. Lu, *Chem. Lett.*, 1996, **9**, 729; P. Lu, T. Teranishi, K. Asakura, M. Miyake and N. Toshima, *J. Phys. Chem. B*, 1999, **103**, 9673.

8 J. C. Bertolini, P. Miegge, P. Hermann, J. L. Rousset and B. Tardy, *Surf. Sci.*, 1995, **331**, 651; P. Hermann, B. Tardy, D. Simon, J. M. Guigner, B. Bigot and J. C. Bertolini, *Surf. Sci.*, 1994, **307**, 422; P. Hermann, D. Simon and B. Bigot, *Surf. Sci.*, 1996, **350**, 301.

9 G. A. Ozin, A. Kuperman and A. Stein, *Angew. Chem., Int. Ed. Engl.*, 1989, **28**, 359 and references therein; G. D. Stucky and J. MacDougall, *Science*, 1990, **247**, 669 and references therein; Y. Wang and N. Herron, *Res. Chem. Int.*, 1991, **15**, 17.

10 J.-L. Malleron, J.-C. Fiaud and J. Y. Legros, *Handbook of Palladium Catalysed Organic Reactions*, Academic Press, San Diego, 1997; J.-L. Malleron and A. Juin, *Database of Palladium Chemistry*, Acadamic Press, San Diego, 1997; L. Xu, G.-D. Lei, W. M. H. Sachtler, R. D. Cörtright and J. A. Dumesic, *J. Phys. Chem.*, 1993, **97**, 11517 and references therein; W. M. H. Sachtler and A. Yu. Stakheev, *Catal. Today*, 1993, **12**, 283 and references therein; Z. Zhang, L. Xu and W. M. H. Sachtler, *J. Catal.*, 1991, **131**, 502; J. H. Sinfelt, *Acc. Chem. Res.*, 1987, **20**, 134; P. Gallezot, in *Metal Clusters*, ed. M. Moskovits, J. Wiley, New York, 1986, pp. 219–247; B. C. Gates, *Catalytic Chemistry*, J. Wiley, New York, 1992; L. L. Moiseev and M. N. Vargaftik, *New J. Chem.*, 1998, **22**, 1217.

11 L. Markó and A. Vizi-Orosz, in *Metal Clusters in Catalysis*, eds. B. C. Gates and H. Knözinger, Elsevier, New York, 1986, p. 89; L. Guczi, in *Metal Clusters in Catalysis*, eds. B. C. Gates and H. Knözinger, Elsevier, New York, 1986, p. 547.

12 M. Lee, SRTC, Westinghouse Savannah River Company, Aiken, South Carolina, personal communication, August 1995.

13 (*a*) G. Longoni, M. Manassero and M. Sansoni, *J. Am. Chem. Soc.*, 1980, **102**, 3242; (*b*) E. Brivio, A. Ceriotti, R. D. Pergola, L. Garlaschelli, F. Demartin, M. Manassero, M. Sansoni, P. Zanello, F. Laschi and B. T. Heaton, *J. Chem. Soc., Dalton Trans.*, 1994, 3237.

14 R. C. B. Copley, C. M. Hill and D. M. P. Mingos, *J. Cluster Sci.*, 1995, **6**, 71.

15 J. W.-S. Hui and W.-T. Wong, *Chem. Commun.*, 1997, 2009.

16 (*a*) M. Kawano, J. W. Bacon, C. F. Campana and L. F. Dahl, *J. Am. Chem. Soc.*, 1996, **118**, 7869; (*b*) M. Kawano, J. W. Bacon, C. F. Campana, B. E. Winger, J. D. Dudek, S. A. Sirchio, S. L. Scruggs, U. Geiser and L. F. Dahl, submitted for publication.

17 J. W. Bacon and L. F. Dahl, unpublished research.

18 M. A. Kozee and L. F. Dahl, manuscript in preparation.

19 M. Kawano and L. F. Dahl, manuscript in preparation.

20 J. M. Bemis and L. F. Dahl, *J. Am. Chem. Soc.*, 1997, **119**, 4545.

21 A. Nash and P. Nash, in *Phase Diagrams of Binary Nickel Alloys*, ed. P. Nash, ASM International, Materials Park, 1991, pp. 251–256 and references therein; M. Hansen and K. Anderko, in *Constitution of Binary Alloys*, McGraw-Hill, New York, 1958, pp. 1029–1032 and references therein.

22 N. T. Tran, M. Kawano, R. K. Hayashi, D. R. Powell, C. F. Campana and L. F. Dahl, *J. Am. Chem. Soc.*, 1999, **121**, 5945.

23 J. Wittayakun, N. T. Tran, D. R. Powell and L. F. Dahl, manuscript in preparation.

24 C. Femoni, M. C. Iapalucci, G. Longoni, P. H. Svensson and J. Wolowska, *Angew. Chem., Int. Ed.*, 2000, **39**, 1635.

25 A. J. Amoroso, L. H. Gade, B. F. G. Johnson, J. Lewis, P. R. Raithby and W.-T. Wong, *Angew. Chem., Int. Ed. Engl.*, 1991, **30**, 107; L. H. Gade, B. F. G. Johnson, J. Lewis, M. J. McPartlin, H. R. Powell, P. R. Raithby and W.-T. Wong, *J. Chem. Soc., Dalton Trans.*, 1994, 521.

26 S. Martinengo, G. Ciani and A. Sironi, *J. Am. Chem. Soc.*, 1980, **102**, 7564.

27 J. Donohue, in *The Structures of the Elements*, John Wiley and Sons, Inc., New York, 1974.

28 Covalent radii are Ni (1.20 Å) and Pd (1.31 Å): W. W. Porterfield, in *Inorganic Chemistry: A Unified Approach*, Addison-Wesley, Reading, 1984, p. 168.

29 D. M. P. Mingos, *J. Chem. Soc., Chem. Commun.*, 1985, 1352; D. M. P. Mingos and L. Zhenyang, *J. Chem. Soc., Dalton Trans.*, 1988, 1657.

30 This model, which presumes that radial interactions dominate in a close-packed metal cluster, states that the total CVE count is given by $\Delta_i + 12\,n_s$, where Δ_i is the central fragment (*viz.* 170 for a centered 13-atom twinned cuboctahedron) and n_s the number of surface atoms (*viz.* 13). The use of this formula gives 326 CVEs.

31 B. K. Teo, H. Zhang, Y. Kean, H. Dang and X. Shi, *J. Chem. Phys.*, 1993, **99**, 2929; B. K. Teo and H. Zhang, *Polyhedron*, 1990, **9**, 1985; B. K. Teo and N. J. A. Sloan, *Inorg. Chem.*, 1986, **25**, 2315.

32 For a close-packed high-nuclearity metal cluster, the topological electron counting rule is given by $N = 2\ T_n = 2\ (6\ G_n + K)$, where N is the number of CVEs, T_n denotes the total number of topological electron pairs, G_n the total number of metal atoms in a close-packed cluster (*viz.* 26) and $K = 7$ because the central atom is surrounded by 12 neighboring atoms in a twinned cuboctahedral arrangement. The resulting number of CVEs is $2T_n = 2\ (6 \times 26 + 7) = 326$.

33 G. J. Miller, *Eur. J. Inorg. Chem.*, 1998, 523 and references therein.

34 B. K. Teo, A. Strizhev, R. Elber and H. Zhang, *Inorg. Chem.*, 1998, **37**, 2482 and references therein.

35 B. K. Teo, H. Zhang and X. Shi, *Inorg. Chem.*, 1994, **33**, 4086; B. K. Teo and H. Zhang, *Coord. Chem. Rev.*, 1995, **143**, 611; H. Zhang and B. K. Teo, *Inorg. Chim. Acta*, 1997, **265**, 213.

36 D. M. P. Mingos and L. Zhenyang, *Comments Inorg. Chem.*, 1989, **9**, 95.

37 See footnote (29) in ref. 22.

38 T. A. Stromnova and I. I. Moiseev, *Russ. Chem. Rev.*, 1998, **67**, 485; S. M. Lee and W. T. Wong, *J. Cluster Sci.*, 1998, **9**, 417; D. M. P. Mingos and R. Vilar, *J. Organomet. Chem.*, 1998, **557**, 131; M. I. Bruce, in *Comprehensive Organometallic Chemistry II*, eds. E. W. Abel, F. G. A. Stone and G. Wilkinson, 1995, vol. 13, pp. 728–752; K. R. Dixon and A. C. Dixon, in *Comprehensive Organometallic Chemistry II*, eds. E. W. Abel, F. G. A. Stone and G. Wilkinson, 1995, vol. 9, pp. 193–223; A. D. Burrows and D. M. P. Mingos, *Transition Met. Chem.*, 1993, **18**, 129; K. C. C. Kharas and L. F. Dahl, *Adv. Chem. Phys.*, 1988, **70** (Part 2), 1; N. K. Eremenko, E. G. Mednikov and S. S. Kurasov, *Russ. Chem. Rev.*, 1985, 394.

39 G. M. Sheldrick, SADABS, Program for empirical absorption correction of area detector data, University of Göttingen, 1996.

40 G. M. Sheldrick, SHELXTL, version 5, 1994, reference manual, Bruker-AXS, 6300 Enterprise Dr., Madison, WI 53719-1173, USA; International Tables for Crystallography, Vol. C, Tables 6.1.1.4, 4.2.6.8, and 4.2.4.2, Kluwer, Boston, MA, 1995.